International Journal of Modern Physics A
© World Scientific Publishing Company

arXiv:hep-ph/0510252v2 8 Nov 2006

LIGHT SUPERPARTNERS AT HADRON COLLIDERS

D.YU. BOGACHEV[2], A.V. GLADYSHEV[1,2,*], D.I. KAZAKOV[1,2,†] and A.S. NECHAEV[2]

[1] *Bogoliubov Laboratory of Theoretical Physics, Joint Institute for Nuclear Research, 141980, 6 Joliot-Curie, Dubna, Moscow Region, Russian Federation*

[2] *Institute for Theoretical and Experimental Physics, 117218, 25 B.Cheremushkinskaya, Moscow, Russian Federation*

Received Day Month Year
Revised Day Month Year

Uncertainties of the MSSM predictions are due to an unknown SUSY breaking mechanism. To reduce these uncertainties, one usually imposes constraints on the MSSM parameter space. Recently, two new constraints became available, both from astrophysics: WMAP precise measurement of the amount of the Dark Matter in the Universe and EGRET data on an excess in diffuse gamma ray flux. Being interpreted as a manifestation of supersymmetry these data lead to severe constraints on parameter space and single out a very restricted area. The key feature of this area is the splitting of light gauginos from heavy squarks and sleptons. We study the phenomenological properties of this scenario, in particular, the cross-sections of superparticle production, their decay patterns and signatures for observation at hadron colliders, Tevatron and LHC. We found that weakly interacting particles in this area are very light so that the cross-sections may reach fractions of a pb with jets and/or leptons as final states accompanied by missing energy taken away by light neutralino with a mass around 100 GeV.

Keywords: Superpartners; Colliders.

PACS numbers:

1. Introduction

Search for supersymmetry at accelerators of the previous decade did not result in discovery of any new physics but rather pushed forward the boundary of unknown territory up to a few hundred GeV. Still the low energy supersymmetry and first of all the MSSM [1,2,3,4,5] proved to be a consistent model compatible with all experimental data and promissing new discoveries round the corner. Numerous attempts to fit the theoretical and experimental requirements with the MSSM have led to a consistent picture of restricted parameter space where prediction of

*e-mail: gladysh@theor.jinr.ru
†e-mail: kazakovd@theor.jinr.ru

the particle spectra and of the cross-sections of supersymmetry production is possible [6,7,8,9,10,11,12,13,14,15,16,17,18]. Though the details depend on the choice of constraints and the mechanism of supersymmetry breaking, the allowed region of parameter space still indicates the presence of light superpartners within the reach of modern accelerators.

The main hopes of the last decade were connected with the LEP II e^+e^- collider, where the light charginos, the superpartners of the weak gauge bosons and charged Higgses, might be produced together with light sleptons, the superpartners of the three generations of leptons. As for the strongly interacting particles, squarks and gluino, they are typically much heavier, at least within mSUGRA models, and the corresponding production cross-sections are suppressed.

The situation has changed after LEP shutdown since now we have the Tevatron and soon coming LHC hadron colliders. There one expects that first of all the strongly interacting particles will be produced because the cross-section is enhanced by the strong coupling. However, the severe background coming from the SM particles is essential and one has a problem in extracting the signal from the background.

Recently, a new ingredient to this scheme came from astroparticle physics where considerable experimental activities, mostly in space, has led to remarkably precise data. In particular, the WMAP collaboration measuring the thermal fluctuations of the Cosmic Microwave Background determined the matter content of the Universe resulting in $23 \pm 4\%$ attributed to the Dark Matter [19,20]. It perfectly fits supersymmetry, since SUSY provides an excellent candidate for the Dark Matter particle, namely, the lightest neutralino, a mixture of the superpartners of the photon, Z-boson and neutral Higgses. Due to a high precision the WMAP data provide a very restrictive constraint on SUSY models, and allow one to further restrict the parameter space.

The other contribution comes from the cosmic ray data. It refers to the measurement of the flux and the spectrum of the gamma rays and antiparticles coming to the Earth. In particular, the diffuse gamma rays were measured in a satellite experiment by the EGRET collaboration and result in an excess above the background for the energies above 1 GeV [21,22,23,24,25,26]. Being interpreted as additional contribution coming from the SUSY Dark Matter annihilation it leads to rather restrictive constraint on the value of the neutralino mass and, respectively, to the restriction on the parameter space of the MSSM [27,28,29,30,31,32].

We show below that taking into account all these constraints results in a very narrow region of the parameter space. Choosing parameters in this region one can calculate the spectrum of superpartners and the cross-section of their production. These cross-sections happen to be relatively large to be of interest for future experiments at hadron colliders. Moreover, as it will be shown below, the cross-section for the chargino production given by the weak processes is unexpectedly high and approaches that for the strong processes of squark and gluino production. This might serve as a signature for supersymmetry in the future LHC experiments.

2. Features of the EGRET preferred region

The framework of our analysis is the Minimal Supersymmetric Standard Model with supergravity inspired supersymmetry breaking terms. The parameters of the model are those of the Standard Model (three gauge couplings α_i, and three 3×3 matrices of the Yukawa couplings y^i_{ab}, where $i = L, U, D.$), Higgs mixing parameter μ, and a set of SUSY breaking parameters (mass terms for squarks and sleptons, mass terms for gauginos and bilinear and trilinear terms).

In the general case, the MSSM contains more than a hundred unknown parameters. Most of them come from the SUSY breaking sector and are the main source of uncertainties. To reduce the number of unknown parameters, one usually imposes some constraints, both simple and obvious, and model-dependent ones.

One of the strictest constraints is the gauge couplings unification, it fixes the threshold of supersymmetry breaking $M_{SUSY} \sim 1$ TeV, thus fixing the scale of superparticle masses [33,34,35]. The second very hard constraint follows from the requirement of radiative electroweak symmetry breaking. While running from the GUT scale towards the lower energies, one (or both) of the Higgs mass-squared parameters $m^2_{H_i}$ becomes negative; thus the condition for spontaneous breaking of electroweak symmetry is fulfilled. Requiring the breaking to take place at the EW scale $M_{EW} \sim 100$ GeV restricts the initial conditions for the corresponding RGE at the GUT scale for the Higgs masses to be equal to $\sqrt{m_0^2 + \mu^2}$, thus expressing the value of the μ parameter in terms of m_0 and $m_{1/2}$. The sign of μ remains undetermined. One can fix it from other constraints, for example, from the anomalous magnetic moment of the muon which has a small deviation from the Standard Model predictions of the order of 2σ. This deficiency may be easily filled with the SUSY contribution, which is proportional to μ. This requires a positive sign of μ that kills a half of the parameter space of the MSSM [36,37,38,39,40,41,42,43].

Further constraints are due to flavour changing processes like $b \to s\gamma$ responsible for the rare B-meson decays which can occur at the one-loop level due to a virtual W-top pair and are strongly suppressed in the Standard Model. In the supersymmetric model contribution to the branching ratio $BR(b \to s\gamma)$ due to superpartners exchange may be rather big, exceeding the experimental value by a few standard deviations. However, the next-to-leading order corrections are essential and improve the situation. This requirement imposes severe restrictions on the parameter space, especially in the case of high $\tan\beta$ [44,45,46,47,48,49,50,51,52,53,54,55,56,57].

Experimental lower limits on the Higgs boson mass [58] impose further constraints when taking into account two-loop radiative corrections. This limit ($m_h \leq 113.4$ GeV) forbids left lower corner of the $m_0 - m_{1/2}$ plane, together with the $b \to s\gamma$ constraint [42,59,60]. Conservation of R-parity results in the existence of the lightest supersymmetric particle (LSP) which is usually the lightest neutralino χ^0_1. The neutralino is a perfect candidate for the non-baryonic cold Dark Matter particle. The requirement that LSP is the lightest neutralino excludes the whole area in the parameter space, where LSP is the charged stau [61,62].

Recent very precise data from WMAP collaboration, which measured thermal fluctuations of Cosmic Microwave Background radiation, restricted the amount of the Dark matter in the Universe up to $23 \pm 4\%$. This imposes further restrictions on the model. In the early Universe all particles were produced abundantly and were in thermal equilibrium through annihilation and production processes. The time evolution of the number density of the particles is given by Boltzmann equation and can be evaluated knowing the thermally averaged total annihilation cross section. The amount of neutralinos should not be too large to overclose the Universe and, at the same time, it should be large enough to produce the right amount of the Dark matter. This serves as a very severe bound on SUSY parameters and leaves a very narrow band in the $m_0 - m_{1/2}$ plane (WMAP-band) [63,64,65,66,67,68].

Having in mind the above mentioned constraints one can find the most preferable region of the parameter space by minimizing the χ^2 function. It is remarkable that all these constraints can be fulfilled simultaneously.

In what follows, we consider the $m_0 - m_{1/2}$ plane and find the allowed region in this plane. Each point at this plane corresponds to a fixed set of parameters and allows one to calculate the spectrum, cross-sections, etc.

New constraints also comes from astrophysics. According to recent data from EGRET collaboration on diffuse gamma ray flux, there is a clear isotropic excess for energies above 1 GeV in comparison with the expectations from conventional galactic models. If one conjectures that it is due to the Dark Matter (neutralino) annihilation, then from the position of the excess one can fit the preferable neutralino mass which happens to be around 80 GeV which in turn restricts the value

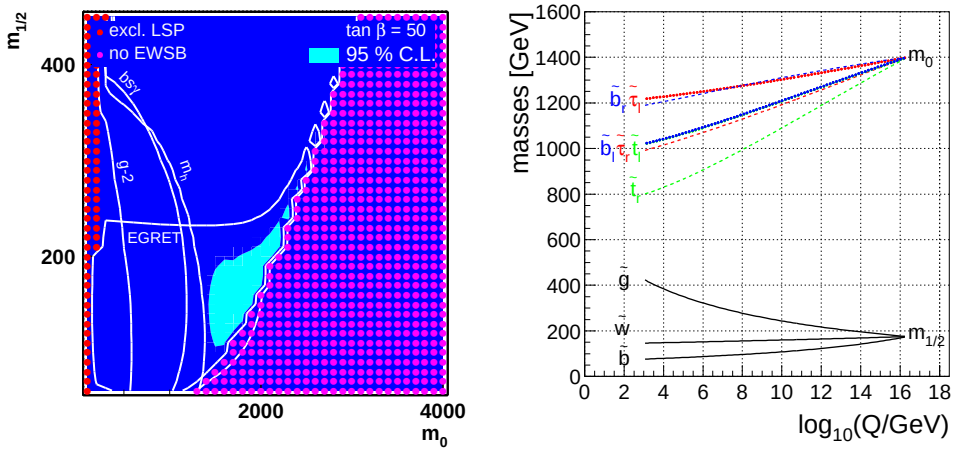

Fig. 1. 1.MSSM parameter space. The light shaded (blue) area is the region preferred by EGRET data for $\tan\beta = 50$, $\mu > 0$ and $A_0 = 0$. The excluded regions where the stau would be the LSP, or EWSB fails, or the Higgs boson is too light are indicated by the dots. 2. Running masses of squarks and gauginos with values of $m_1/2$ and m_0 compatible with EGRET data.

of $m_{1/2}$. It appears that the most preferable values are about $m_{1/2} = 180$ GeV and $m_0 \simeq 1400$ GeV (Fig.1).

This region has not been intensively studied yet, though it is within the reach of Tevatron and forthcoming LHC. It appears to be very interesting phenomenologically, because of the mass splitting between light gauginos and heavy squarks and sleptons (see Fig.1 right). The cross-sections for chargino and neutralino production in this case are relatively large not being suppressed by masses and being comparable with squark and gluino production. The latter being enhanced by strong interactions remains suppressed by heaviness of squarks. This means that in the EGRET region leptonic channels are not suppressed and so might give clear leptonic signature for supersymmetry in the upcoming LHC experiments. Below we study these cross-sections and the main decay modes in detail.

3. Neutralino and chargino production and decay modes

Owing to small $m_{1/2}$ and large m_0 in the chosen region of parameter space we deal with relatively light gauginos and heavy squarks (Fig.1). Charginos and neutralinos are, respectively, two and four eigenstates of the corresponding mass matrices. The neutralino mass matrix is

$$M^{(0)} = \begin{pmatrix} M_1 & 0 & -M_Z c_\beta s_W & M_Z s_\beta s_W \\ 0 & M_2 & M_Z c_\beta c_W & -M_Z s_\beta c_W \\ -M_Z c_\beta s_W & M_Z c_\beta c_W & 0 & -\mu \\ M_Z s_\beta s_W & -M_Z s_\beta c_W & -\mu & 0 \end{pmatrix}, \tag{1}$$

where $c_\beta = \cos\beta$, $s_\beta = \sin\beta$. s_W and c_W are the sine and cosine of the Weinberg angle respectively. Four eigenstates of this matrix are the four types of physical particles. The lightest one $\tilde{\chi}_1^0$, is the LSP. In the chosen region of small $m_{1/2}$ the lightest neutralino mass is around 70 GeV which perfectly fits the EGRET data. For $m_{1/2} = 180$ GeV the values of gaugino masses are $M_1 = 120$ GeV and $M_2 = 250$ GeV.

The lightest neutralino in our case is mostly bino, the second neutralino is mostly wino, while the third and the fourth are mostly higgsinos (see Table 1).

Two egienstates of the chargino mass matrix

$$M^{(c)} = \begin{pmatrix} M_2 & \sqrt{2} M_W s_\beta \\ \sqrt{2} M_W c_\beta & \mu \end{pmatrix}. \tag{2}$$

Table 1. The bino, wino, first and second higgsino fractions of neutralinos.

	Bino	Wino	1st higgsino	2nd higgsino	mass (GeV)
χ_1^0	90%	1%	8%	1%	70
χ_2^0	5%	71%	18%	6%	125
χ_3^0	1%	2%	46%	51%	220
χ_4^0	3%	25%	30%	42%	250

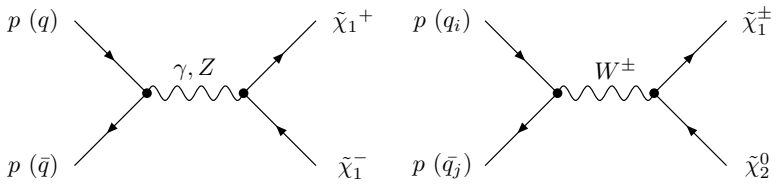

Fig. 2. Leading chargino and neutralino production processes.

are the two charginos $\tilde{\chi}^{\pm}_{1,2}$. Their masses are given by the following formula:

$$M^2_{1,2} = \frac{1}{2}\Big[M_2^2+\mu^2+2M_W^2 \mp \sqrt{(M_2^2-\mu^2)^2+4M_W^4\cos^2 2\beta+4M_W^2(M_2^2+\mu^2+2M_2\mu\sin 2\beta)}\Big] \quad (3)$$

The first chargino is relatively light due to the gaugino component.

To calculate the cross-sections for sparticle production at hadron colliders we use the CalcHEP 2.3.7. package [69] which takes into account parton distributions inside protons [70]. First we selected three leading types of chargino and neutralino production processes (Fig. 2).

The calculations are made for proton-proton collisions at the center of mass energy of $\sqrt{s} = 14$ TeV (LHC). As one can see from Fig. 3, the cross sections for neutralino and chargino production processes slightly depend on m_0 and strongly depend on $m_{1/2}$; thus, for the future reference we fix the value of $m_0 = 1400$ GeV.

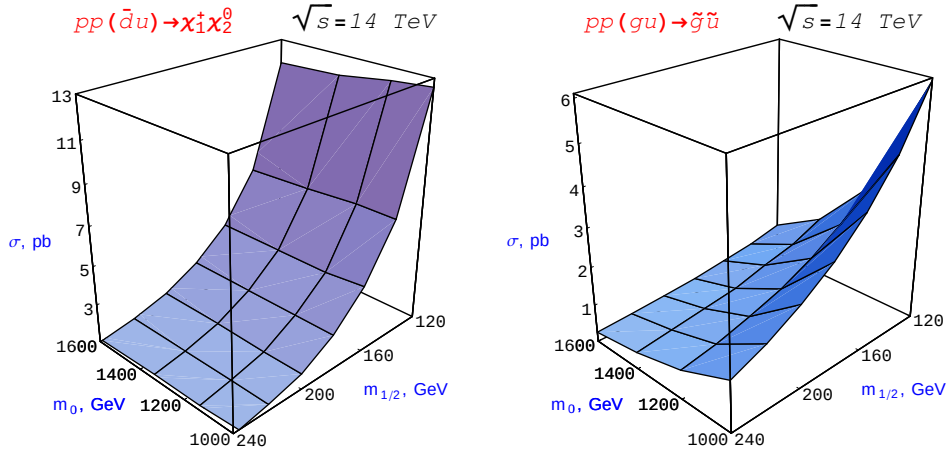

Fig. 3. The cross-section for chargino and neutralino production at LHC for $\sqrt{s} = 14$ TeV as functions of $m_{1/2}$ and m_0 for $\tan\beta = 51$, $A_0 = 0$ and sign(μ)=1.

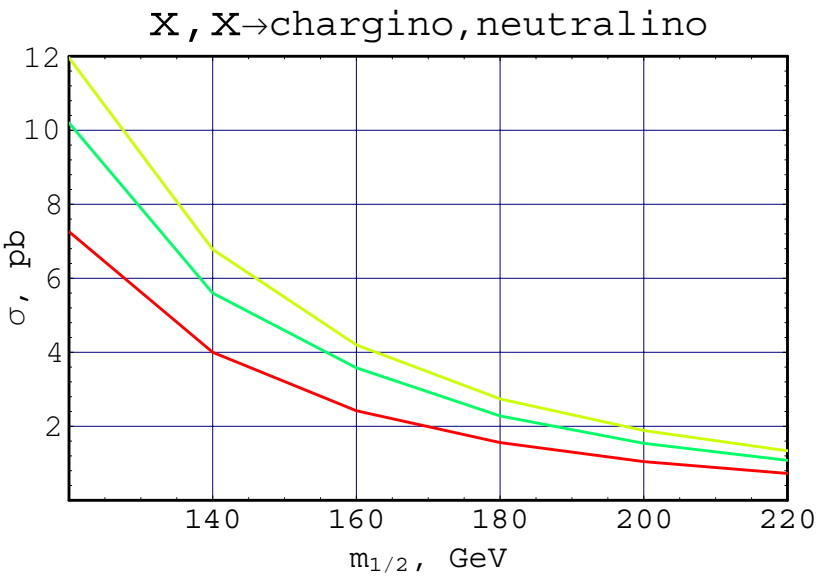

Fig. 4. The cross-section dependence on $m_{1/2}$ for chargino and neutralino production. The upper yellow line is for $pp(q\bar{q}) \to \tilde{\chi}_2^0\tilde{\chi}_1^+ + X$, the red line in the bottom is for $pp(q\bar{q}) \to \tilde{\chi}_2^0\tilde{\chi}_1^- + X$, and the green line in the middle is for $pp(q\bar{q}) \to \tilde{\chi}_1^+\tilde{\chi}_1^- + X$ in case of $m_0 = 1400$ GeV, $\tan\beta = 51$, $A_0 = 0$ and sign(μ)=1.

The cross section dependence on $m_{1/2}$ for chargino and neutralino production processes is shown in Fig.4.

In this region of parameter space the cross section for production of the second neutralino alongside with the first chargino is larger, owing to the mixing parameters, than that when the lightest neutralino is produced. After being produced the light chargino and the second neutralino rapidly decay into the Standard Model particles and the LSP. The decay modes and partial widths obtained from ISAJET [71] are shown in Table 2.

Chargino mostly decays into LSP and via virtual W boson into either quarks of different flavor or a neutrino–lepton pair. The second neutralino decays into LSP

Table 2. The 1st chargino and the 2nd neutralino decay modes and partial widths for $m_0 = 1400$ GeV, $m_{1/2} = 180$ GeV, $\tan\beta = 51$, $A_0 = 0$ and sign(μ)=1.

Initial particle	Decay mode	Branching ratio	Partial width (GeV)
$\chi_1^\pm$	$\chi_1^0\ \bar{q}_i\ q_k$	67%	0.35×10^{-4}
	$\chi_0^1\ \ell\ \nu$	33%	0.17×10^{-4}
χ_2^0	$\chi_1^0\ q\ \bar{q}$	70%	0.66×10^{-5}
	$\chi_1^0\ \bar{\ell}\ \ell$	10%	0.10×10^{-5}
	$\chi_1^0\ \bar{\nu}\ \nu$	20%	0.20×10^{-5}

Table 3. Production of the 1st chargino and the 2nd neutralino with subsequent cascade decays.

Process	Final states	Process	Final states
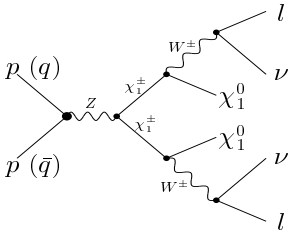	2ℓ 2ν $\not{E}_T$ $\sigma \approx 0.25$ pb	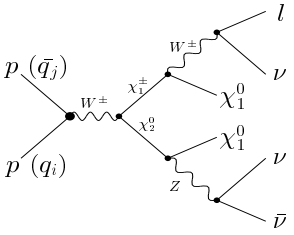	ℓ 3ν $\not{E}_T$ $\sigma \approx 0.28$ pb
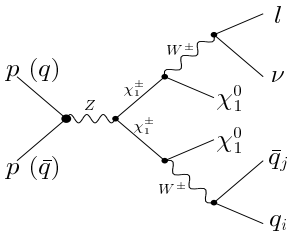	ℓ ν $2j$ $\not{E}_T$ $\sigma \approx 0.50$ pb	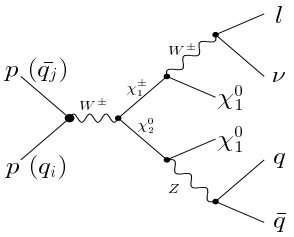	ℓ ν $2j$ $\not{E}_T$ $\sigma \approx 1.0$ pb
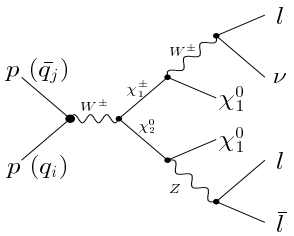	3ℓ ν $\not{E}_T$ $\sigma \approx 0.14$ pb	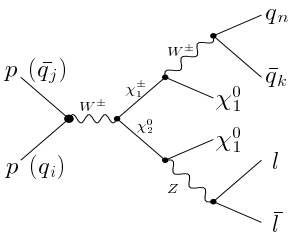	2ℓ $2j$ $\not{E}_T$ $\sigma \approx 0.29$ pb

and via virtual Z-boson into either quark–antiquark pair or lepton–antilepton pair. Different types of chargino and neutralino cascade decays are shown in Table 3.

Thus, in the chosen region of parameter space due to the relatively large neutralino and chargino production cross sections and branching ratios to leptons and LSP, one can have an unexpectedly large number of outgoing leptons. Moreover, some of the pure leptonic events, like one or three charged leptons clearly differ from the Standard Model background (pair W and Z production) by *large* missing energy, thus being a convincing indication to the new physics.

The same analysis was conducted for the proton-antiproton collisions at the Tevatron center of mass energy $\sqrt{s} = 2$ TeV. The Tevatron energy is not sufficient to produce heavy squarks or sleptons but is sufficient to produce light charginos and neutralinos. The cross-section dependence for chargino pair production on $m_{1/2}$ is shown in Fig. 5. As one can see the cross-section is around 0.1–1 pb. The chargino has the same decay modes as discussed above but ten times smaller cross section compared to LHC. However, the present Tevatron luminosity is not enough to extract the signal from the background, and one can get only lower limits on chargino masses (117 GeV at the 95% C.L.) [72].

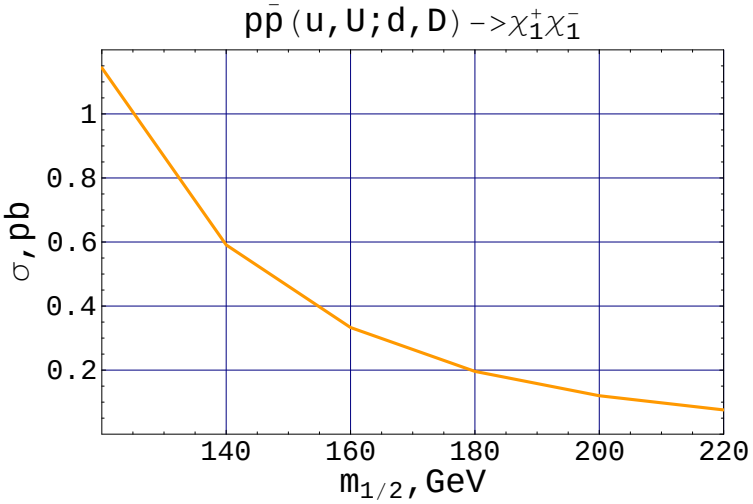

Fig. 5. Cross section dependence on $m_{1/2}$ for chargino pair production $p\bar{p} \to \chi_1^+ \chi_1^-$ at TeVatron for $m_0 = 1400$ GeV, $\tan\beta = 51$, $A_0 = 0$ and sign(μ)=1.

4. Squark and gluino production and decay modes

Squarks of the 3rd generation are two eigenstates of the mass matrices

$$\begin{pmatrix} \tilde{m}_{tL}^2 & m_t(A_t - \mu \cot\beta) \\ m_t(A_t - \mu \cot\beta) & \tilde{m}_{tR}^2 \end{pmatrix}, \tag{4}$$

$$\begin{pmatrix} \tilde{m}_{bL}^2 & m_b(A_b - \mu \tan\beta) \\ m_b(A_b - \mu \tan\beta) & \tilde{m}_{bR}^2 \end{pmatrix}, \tag{5}$$

where

$$\begin{aligned} \tilde{m}_{tL}^2 &= \tilde{m}_Q^2 + m_t^2 + \frac{1}{6}(4M_W^2 - M_Z^2)\cos 2\beta, \\ \tilde{m}_{tR}^2 &= \tilde{m}_U^2 + m_t^2 - \frac{2}{3}(M_W^2 - M_Z^2)\cos 2\beta, \\ \tilde{m}_{bL}^2 &= \tilde{m}_Q^2 + m_b^2 - \frac{1}{6}(2M_W^2 + M_Z^2)\cos 2\beta, \\ \tilde{m}_{bR}^2 &= \tilde{m}_D^2 + m_b^2 + \frac{1}{3}(M_W^2 - M_Z^2)\cos 2\beta. \end{aligned} \tag{6}$$

The first terms here are the soft SUSY breaking parameters, the second terms are the ordinary quark masses and the third ones are the so called D-terms. Similar formulae can be written for the first and second generations.

The nonvanishing Yukawa couplings result in the large mixing and splitting of mass eigenstates for the third generation of squarks. As a result one of the eigenstates becomes lighter than the others. This leads to a remarkable consequence: the decay branching ratios for the third generation of squarks are several times bigger than those for the first two generations as we will discuss below.

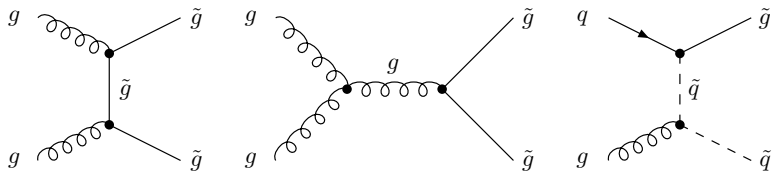

Fig. 6. Leading types of strongly interacting sparticles production processes.

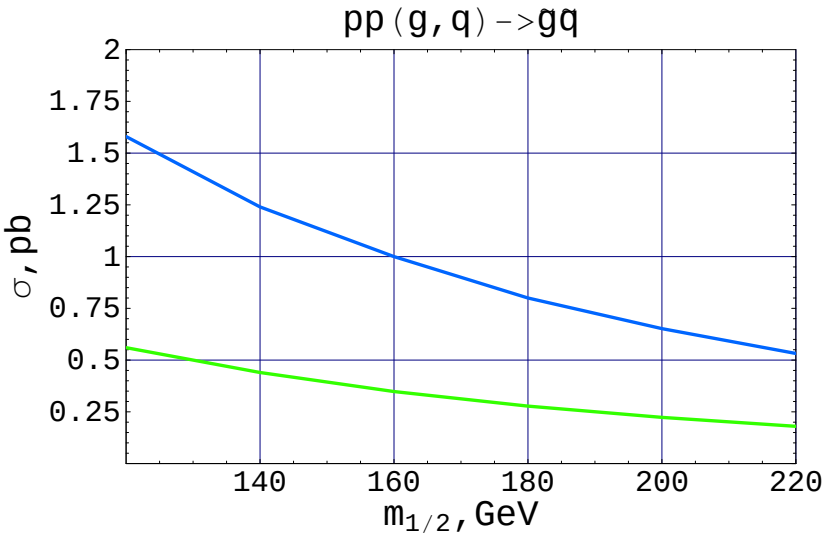

Fig. 7. Cross-section for squark production as a function of $m_{1/2}$. The upper blue line is for $pp\ (q\bar{q}) \to \tilde{g}\tilde{u} + X$, the purple line in the bottom is for $pp\ (q\bar{q}) \to \tilde{g}\tilde{d} + X$ in case of m_0=1400 GeV $\tan\beta = 51$, $A_0 = 0$ and sign(μ)=1.

The cross-sections for squark production via proton collisions at the center of mass energy of $\sqrt{s} = 14$ TeV are strongly suppressed due to the large squark masses. At the same time, the cross-sections for squark-gluino and pair gluino production are not that strongly suppressed due to the relatively light gluino. The leading procceses for production of strongly interacting spacticles are shown in Fig. 6.

The cross-sections for squark and gluino production depend on $m_{1/2}$ much stronger than on m_0. As it was mentioned above we fixed the value of $m_0 = 1400$ GeV. The dependence of squark and gluino production cross-section on $m_{1/2}$ is shown in Fig. 7.

One can see that the cross-section for squark and gluino production is of the same order of magnitude as the cross section for chargino and neutralino production. However, further squarks and gluinos are the main source of outgoing jets in sparticle decay while charginos and second neutralinos are the main source of leptons.

At the same time, in the small $m_{1/2}$ region light gluino production cross-section

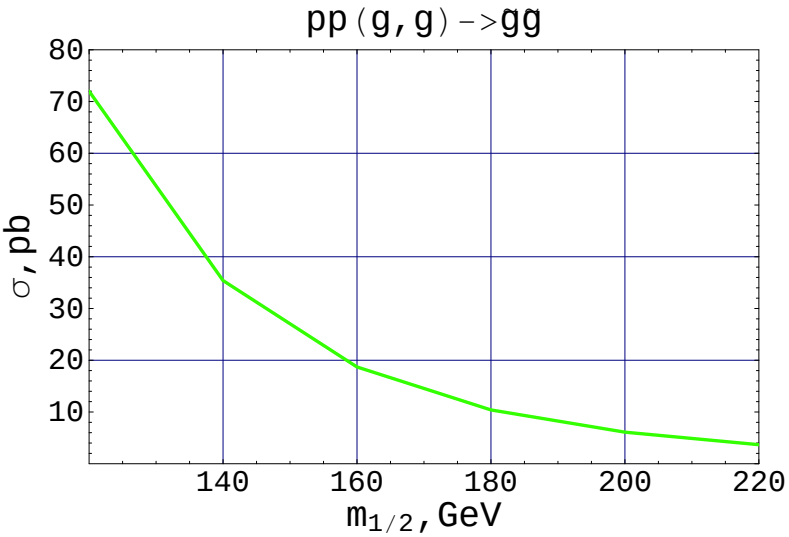

Fig. 8. Cross-section for gluino production $pp\ (gg) \to \tilde{g}\tilde{g} + X$ as a function of $m_{1/2}$ in case of m_0=1400 GeV $\tan\beta = 51$, $A_0 = 0$ and sign(μ)=1.

in proton collisions via gluon fusion (Fig. 8) is by almost two orders of magnitude larger than all other sparticle production cross-sections.

After being produced gluinos rapidly decay. Different types of gluino decay modes obtained from ISAJET [71] are shown in Table 4. There are two leading decay modes. First of them is when gluino decays to bottom quark and via virtual sbottom into the second neutralino and anti-bottom quark, while in the second case it decays into quark and via virtual squark to the first chargino and anti-quark of a different flavor. Charginos and neutralinos produced in gluino decay processes may decay not only to quarks but also to leptons. Hence, gluino cascade decays might have a different number of leptons and jets in the final states, as shown in Table 5. This slightly differs chargino and neutralino decays which have pure leptonic final states.

As one can see from Fig. 9, the cross-sections for all sparticle production pro-

Table 4. Gluino and top-quark decay modes and partial widths.

Initial particle	Decay mode	Branching ratio	Partial width (GeV)
$\tilde{g}$	$\chi_2^0\ \bar{b}\ b$	16%	0.14×10^{-4}
	$\chi_2^0\ \bar{q}\ q$	24%	0.20×10^{-4}
	$\chi_1^\pm\ \bar{q}_i\ q_k$	30%	0.27×10^{-4}
	$\chi_1^\pm\ \bar{t}\ b$	6.6%	0.55×10^{-4}
t	$b\ \bar{q}_i\ q_k$	67%	0.8
	$b\ \ell\ \nu$	33%	0.4

Table 5. Cascade decays for pair of gluinos.

Process	Final states	Process	Final states
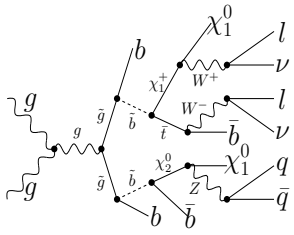	2ℓ 2ν $6j$ $\not{E}_T$ $\sigma \approx 0.008$ pb	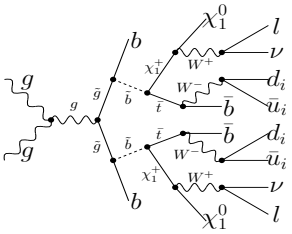	2ℓ 2ν $8j$ $\not{E}_T$ $\sigma \approx 0.002$ pb
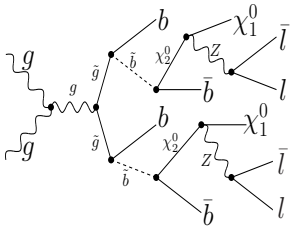	4ℓ $4j$ $\not{E}_T$ $\sigma \approx 0.003$ pb	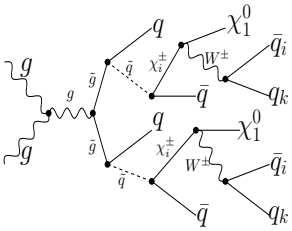	$8j$ $\not{E}_T$ $\sigma \approx 0.40$ pb
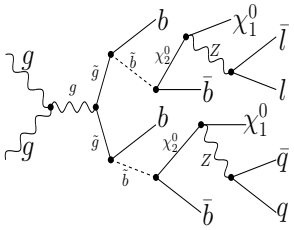	2ℓ $6j$ $\not{E}_T$ $\sigma \approx 0.019$ pb	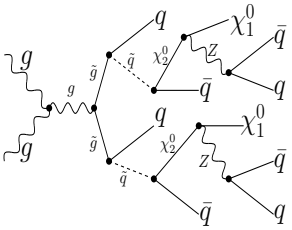	$8j$ $\not{E}_T$ $\sigma \approx 0.29$ pb

cesses drop drastically with increase of $m_{1/2}$. This is especially true for the production processes of weakly interacting sparticles: charginos and second neutralinos due to the large gaugino fraction. Alongside with them drops the number of leptonic events above the Standard Model background. With increase of $m_{1/2}$ gluino production cross-section also becomes suppressed by heavy gluino mass. Most of the final state cross-sections in gluino cascade decays with a variety of leptons and jets in the final states also drop by $2-3$ orders of magnitude with the increase of $m_{1/2}$ up to 400 GeV.

Thus, it looks like only a small $m_{1/2}$ region might bring a relatively large number of leptoninc events coming above the SM background. Moreover, from the analysis conducted for the Tevatron (see Fig. 5) in this region of parameter space supersymmetry is already within a reach of the modern hadron colliders and the only reason why it is not seen is the low luminosity of the Tevatron.

Remarkable that in jet production one mainly has b-jets with the branching ratio that may reach 30 %. This fact finds its explanation in kinematic factors due to the fact that b-squarks are lighter than those of the first two generations.

Indeed, consider the process of gluino decay into quarks and squarks. There are

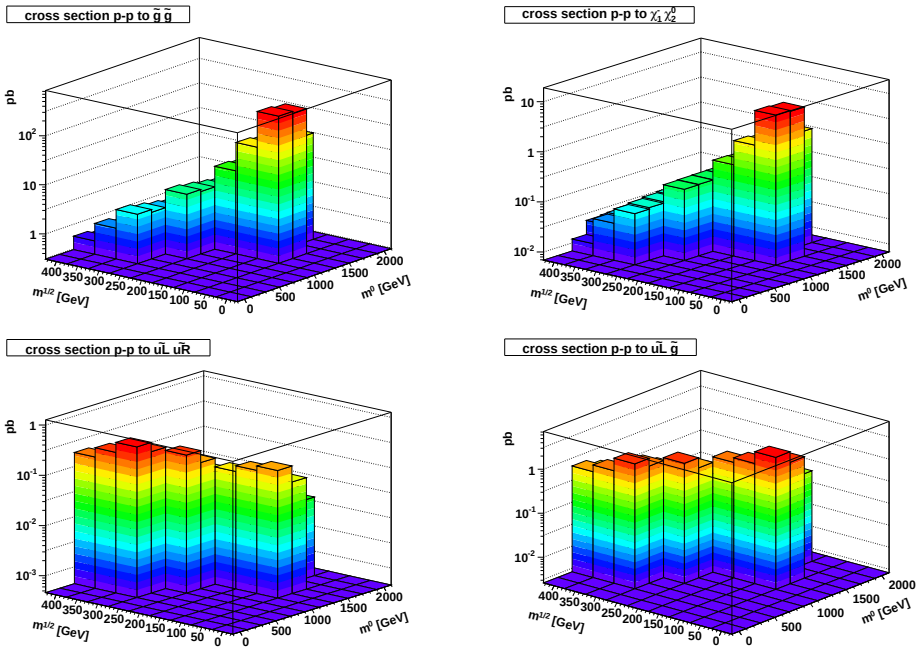

Fig. 9. Cross-section dependence on $m_{1/2}$, m_0 for sparticle production processes for $\tan\beta = 51$, $A_0 = 0$ and sign(μ)=1.

two possibilities: either gluino is heavier than squarks and can decay on the mass shell (see Fig.10a) or it is lighter than squarks and decays into virtual squark which in turn decays into the second neutralino and the quark (see Fig.10b).

In the first case, the width is easily calculable and has the form

$$\Gamma(\tilde{g} \to \tilde{q}q) \sim \frac{1}{m_{\tilde{g}}^3}\sqrt{(m_{\tilde{g}}^2-(m_q-m_{\tilde{q}})^2)(m_{\tilde{g}}^2-(m_q+m_{\tilde{q}})^2)} \times (m_{\tilde{q}}^2 - m_{\tilde{g}}^2 - m_q^2 \pm 2\sin 2\theta_q m_{\tilde{g}} m_q), \quad (7)$$

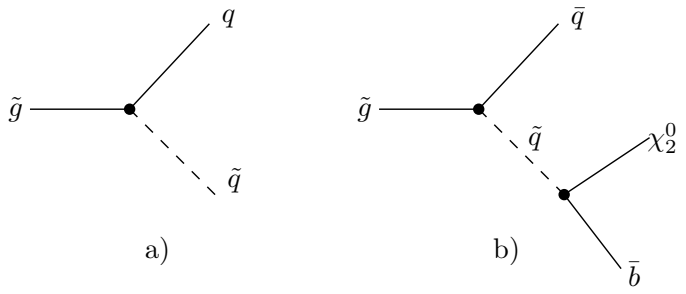

Fig. 10. Leading modes of gluino decay.

where θ_q is the squark mixing angle proportional to the quark mass according to eq.(7) and $\pm$ sign refers to the first and the second squark, respectively. The square root in this equation essentially comes from the phase space.

Since the quark mass is much smaller than the squark one and can be ignored (except for the t quark), eq.(7) can be reduced to

$$\Gamma(\tilde{g} \to \tilde{q}q) \sim (m_{\tilde{g}}^2 - m_{\tilde{q}}^2)^2, \tag{8}$$

which clearly shows that the lighter the squark, the bigger the width. Since the third generation of squarks is lighter than the first two (mainly due to the RG running induced by Yukawa couplings and the mixing in squark mass matrix), the width for the third generation is larger. Besides, the top quark production is suppressed compared to the bottom one due to the large top mass which decreases the phase space in eq.(7). So the b-quark production is enhanced compared to other flavours.

The situation is somewhat different in the second case, when gluino is lighter than squark, which is the case of the EGRET point. Here the expression for the width is more complicated to be written explicitly [73]; however, one can examine the essential part. When gluino is almost on the mass shell, a contribution to the amplitude is proportional to

$$\Gamma(\tilde{g} \to \tilde{q}q\chi_0^2)) \sim \frac{3-body\ phase\ space}{(m_{\tilde{q}}^2 - (m_{\tilde{g}} + m_q)^2)^2}. \tag{9}$$

One can see that the bracket in the denominator which comes from the squark propagator is minimized for the lightest squark, since contrary to the previous case gluino is light. Thus it gives the largest contribution for the third generation for the same reason as above. The contribution to the top quark compared to the bottom one is suppressed due to the phase space which contains only light particles and is essentially reduced for the heavy top.

This way one can justify that in jet production b-jets are dominant in both cases, which sounds promising for experimental observation.

5. Conclusion

Thus, we conclude that in the EGRET preferred region of parameter space of the MSSM (small $m_{1/2} \sim 180$ GeV and large $m_0 \sim 1400$ GeV) characterized by a considerable splitting between the scalar superpartners and gauginos, the cross-sections for sparticle production at hadronic machines may reach a few % pb. Their decay modes lead to jets (mostly b) and/or leptons in the final states with additional missing energy carried by escaping neutralinos. These events have an exceptional signature (see e.g. Table 5) that allows one to distinguish them from the SM background providing enough integrated luminosity and may be promising for SUSY searches within the advocated scenario.

Acknowledgements

Financial support from RFBR grant # 05-02-17603, grant of the Ministry of Science and Technology Policy of the Russian Federation # 5362.2006.2, DFG grant # 436 RUS 113/626/0-1 and the Heisenberg-Landau Programme are kindly acknowledged. We would like to thank W. de Boer, V. Zhukov, and V. Bednyakov for valuable discussions, and A. Pukhov for providing us with the latest version of CalcHEP and for numerical consultations.

Appendix A. Cross-section of a cascade decay

Calculation of cross sections for complex cascade processes is a complicated task if done directly. To simplify it, one can use the following simple trick: one calculates the cross-section of the original $2 \to 2$ process and then just multiplies it by the branching ratios for the corresponding unstable particles at each junction [74].

To justify this algorithm, we demonstrate below how it works for a sample process shown in Fig.11. We have an interaction of two particles with momenta p_1 and p_2 producing two other particles with momenta p' and p, respectively. The particle with momentum p is unstable and decays into two particles with momenta q_1 and q_2.

The cross section of this process is given by

$$d\sigma = \frac{1}{2E_1 2E_2 |v_1 - v_2|} \left(\prod_f \frac{d^3 p_f}{(2\pi)^3 2E_f} \right) |M|^2 (2\pi)^4 \delta^4 (p_1 + p_2 - \sum p_f). \quad \text{(A.1)}$$

The matrix element for this kind of a process looks like

$$M \sim \bar{u}(q_1)\bar{u}(q_2) V_2 D(p) \bar{u}(p') V_1 u(p_1) u(p_2) \delta^4 (q_1 + q_2 - p) d^4 p, \quad \text{(A.2)}$$

where $u(p)$ corresponds to the external particle and equals $1, u_\alpha(p)$ and ϵ_μ for a scalar, spinor and vector particle, respectively, and $D(p)$ is a propagator of an unstable particle with momentum p which we take in the form

$$D(p) = \frac{s(p)}{p^2 - m^2 + im\Gamma}$$

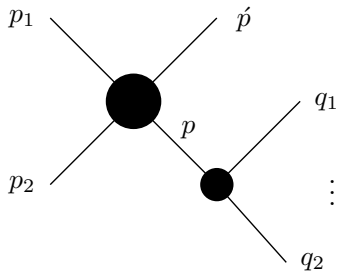

Fig. 11. The cascade process with unstable particle decay.

Here Γ is the total width of an unstable particle and $s(p)$ is a spin dependent part.

To calculate the cross-section, one has to take the square of the matrix element and evaluate the phase space integral. One has

$$
\begin{aligned}
&d\sigma \sim \\
&\frac{1}{(2\pi)^5}|\bar{u}(q_1)\bar{u}(q_2)V_2D(p)\bar{u}(p')V_1u(p_1)u(p_2)\bar{u}(p_2)\bar{u}(p_1)V_1^*u(p')D^*(l)V_2^*u(q_1)u(q_2)| \\
&\times\ \delta^4(q_1+q_2-p)\delta^4(q_1+q_2-l)d^4pd^4l\delta^4(p_1+p_2-p'-q_1-q_2)\frac{d^3q_1d^3q_2d^3p'}{2E_{q1}2E_{q2}2E_{p'}} \\
&=\frac{1}{(2\pi)^5}\frac{|\bar{u}(q_1)\bar{u}(q_2)V_2s(p)\bar{u}(p')V_1u(p_1)u(p_2)|^2}{(p^2-m^2)^2+m^2\Gamma^2}\delta^4(p-q_1-q_2)d^4p \\
&\times\ \delta^4(p_1+p_2-p'-p)\frac{d^3q_1d^3q_2d^3p'}{2E_{q1}2E_{q2}2E_{p'}} \qquad \text{(A.3)}
\end{aligned}
$$

When $\Gamma \ll m$, which means that the particle is relatively stable and is almost on mass shell, one can use the approximate formula

$$\frac{1}{(p^2-m^2)^2+m^2\Gamma^2} \approx \frac{\pi}{m\Gamma}\delta(p^2-m^2). \qquad \text{(A.4)}$$

This is the first step of approximation. Substituting it into eq.(A.3) one gets

$$
\begin{aligned}
d\sigma \sim\ &\frac{1}{(2\pi)^5}|\bar{u}(q_1)\bar{u}(q_2)V_2s(p)\bar{u}(p')V_1u(p_1)u(p_2)|^2\frac{\pi}{m\Gamma}\delta(p^2-m^2) \\
&\times\ \delta^4(p-q_1-q_2)\delta^4(p_1+p_2-p'-p)d^4p\frac{d^3q_1d^3q_2d^3p'}{2E_{q1}2E_{q2}2E_{p'}} \qquad \text{(A.5)}
\end{aligned}
$$

Now one can use the relation

$$\delta(p^2-m^2)d^4p = \frac{d^3p}{2p_0},$$

that gives

$$
\begin{aligned}
d\sigma \sim\ &\frac{1}{(2\pi)^5}|\bar{u}(q_1)\bar{u}(q_2)V_2s(p)\bar{u}(p')V_1u(p_1)u(p_2)|^2\frac{\pi}{m\Gamma} \\
&\times\ \delta^4(p_1+p_2-p'-p)\frac{d^3p\,d^3p'}{2E_p2E_{p'}}\delta^4(p-q_1-q_2)\frac{d^3q_1d^3q_2}{2E_{q1}2E_{q2}} \qquad \text{(A.6)}
\end{aligned}
$$

Now we have to transform the matrix element. It is factorized exactly in the case of a scalar intermediate unstable particle, while in the case of a spinor or vector particle, factorization holds only approximately. One has

$$|\bar{u}(q_1)\bar{u}(q_2)V_2s(p)\bar{u}(p')V_1u(p_1)u(p_2)|^2 \approx |\bar{u}(q_1)\bar{u}(q_2)V_2u(p)|^2|\bar{u}(p')\bar{u}(p)V_1u(p_1)u(p_2)|^2$$

This is the second step of approximation. Thus, the cross-section is factorized into two parts

$$d\sigma_1 \sim \frac{1}{(2\pi)^2}|\bar{u}(p')\bar{u}(p)V_1u(p_1)u(p_2)|^2\delta^4(p_1+p_2-p'-p)\frac{d^3p\,d^3p'}{2E_p2E_{p'}} \qquad \text{(A.7)}$$

and

$$d\Gamma = \frac{1}{(2\pi)^2}|\bar{u}(q_1)\bar{u}(q_2)V_2 u(p)|^2\delta^4(p-q_1-q_2)\frac{d^3q_1 d^3q_2}{2E_p 2E_{q1}2E_{q2}}, \tag{A.8}$$

so that one can write

$$d\sigma = d\sigma_1 d\Gamma \frac{E_p}{m\Gamma}. \tag{A.9}$$

Remind now that for a decaying particle with momentum p, its lifetime is given by:

$$\tau = \frac{1}{\Gamma_{tot}} = \frac{E_p}{m\Gamma}.$$

This finally gives the desired relation

$$d\sigma = d\sigma_1 \frac{d\Gamma}{\Gamma_{tot}}. \tag{A.10}$$

Thus, we finally come to the conclusion that for cascade decays the total cross-section can be obtained by multiplying the original two-particle one by the branching ratios for each unstable particle.

References

1. H.P. Nilles, *Phys. Rept.* **110**, 1 (1984).
2. H.E. Haber and G.L. Kane, *Phys. Rept.* **117**, 75 (1985).
3. H.E. Haber, *Introductory Low-Energy Supersymmetry*, Lectures given at TASI 1992, (SCIPP 92/33, 1993), `hep-ph/9306207`.
4. D.I. Kazakov, *Beyond the Standard Model: in Search of Supersymmetry*, Lectures at the European School of High-Energy Physics 2000, `hep-ph/0012288`.
5. D.I. Kazakov, *Beyond the Standard Model*, Lectures at the European School of High-Energy Physics 2004, `hep-ph/0411064`.
6. L.E. Ibáñez and G.G. Ross, *Nucl. Phys. B* **368**, 3 (1992).
7. G.G. Ross and R.G. Roberts, *Nucl. Phys. B* **377**, 571 (1992).
8. S. Kelley, J.L. Lopez and D.V. Nanopoulos, *Phys. Lett. B* **274**, 387 (1992).
9. V. Barger, M.S. Berger, P. Ohmann and R. Phillips, *Phys. Lett. B* **314**, 351 (1993).
10. V. Barger, M.S. Berger and P. Ohmann, *Phys. Rev. D* **49**, 4908 (1994).
11. P. Langacker and N. Polonsky, *Phys. Rev. D* **49**, 1454 (1994).
12. W. de Boer, R. Ehret and D.I. Kazakov, *Z. Phys. C* **67** 647 (1995).
13. W. de Boer *et al.*, *Z. Phys. C* **71**, 415 (1996).
14. D.M. Pierce, J.A. Bagger, K.T. Matchev and R. Zhang, *Nucl. Phys. B* **491**, 3 (1997).
15. J.R. Ellis, D. Nanopoulos and K. Olive, *Phys. Lett. B* **508**, 65 (2001).
16. J.R. Ellis, T. Falk, G. Ganis, K.A. Olive and M. Srednicki, *Phys. Lett. B* **510**, 236 (2001).
17. H. Baer, C. Balazs, A. Belyaev, J.K. Mizukoshi, X. Tata and W. Wang, *JHEP* **0207**, 050 (2002).
18. H. Baer, C. Balazs, A. Belyaev, T. Krupovnicas and X. Tata, *JHEP* **0306**, 054 (2003).
19. C.L. Bennett *et al.*, *Astrophys. J. Suppl.* **148**, 1 (2003).
20. D.N. Spergel *et al.*, *Astrophys. J. Suppl.* **148**, 175 (2003).
21. E.B. Hughes *et al.*, *IEEE Trans. Nucl. Sci.* **NS-27**, 364 (1980).
22. G. Kanbach, *Space Sci. Rev.* **49**, 69 (1988).
23. D.J. Thompson *et al.*, *Astrophys. J. Suppl.* **86**, 629 (1993).

24. D.L. Bertsch *et al.*, *Astrophys. J.* **416**, 587 (1993).
25. EGRET Collab. (R.C. Hartman *et al.*), *Astrophys. J. Suppl.* **123**, 79 (1999).
26. EGRET public data archive, `ftp://cossc.gsfc.nasa.gov/compton/data/egret/`.
27. W. de Boer, M. Harold, C. Sander and V. Zhukov, *Eur. Phys. J. C* **33**, 981 (2004).
28. W. de Boer, M. Harold, C. Sander, V. Zhukov, A.V. Gladyshev and D.I. Kazakov, `astro-ph/0408272`.
29. W. de Boer, `hep-ph/0508108`.
30. W. de Boer, C. Sander, V. Zhukov, A.V. Gladyshev and D.I. Kazakov, *Astronomy and Astrophysics* **444**, 51 (2005).
31. W. de Boer, C. Sander, V. Zhukov, A.V. Gladyshev and D.I. Kazakov, *Phys. Rev. Lett.* **95**, 209001 (2005).
32. W. de Boer, C. Sander, V. Zhukov, A.V. Gladyshev and D.I. Kazakov, *Phys. Lett. B* **636**, 13, (2006).
33. J.R. Ellis, S. Kelley and D.V. Nanopoulos, *Phys. Lett. B* **260**, 131 (1991).
34. U. Amaldi, W. de Boer and H. Furstenau, *Phys. Lett. B* **260**, 447 (1991).
35. C. Giunti, C.W. Kim and U.W. Lee, *Mod. Phys. Lett. A* **6**, 1745 (1991).
36. G.W. Bennett *et al.*, *Phys. Rev. Lett.* **92**, 161802 (2004).
37. M. Davier, S. Eidelman, A. Hocker and Z. Zhang, *Eur. Phys. J. C* **31**, 503 (2003).
38. K.Hagiwara, A.D.Martin, D.Nomura and T.Teubner, *Phys. Rev. D* **69**, 093003 (2004).
39. J.F. de Troconiz and F.J. Yndurain, *Phys. Rev. D* **71**, 073008 (2005).
40. K. Melnikov and A. Vainshtein, *Phys. Rev. D* **70**, 113006 (2004).
41. M. Passera, *J. Phys. G* **31**, R75 (2005).
42. W. de Boer, M.Huber, C.Sander and D.I. Kazakov, *Phys. Lett. B* **515**, 283 (2001).
43. W. de Boer, M. Huber, C. Sander, A.V. Gladyshev and D.I. Kazakov, A global fit to the anomalous magnetic moment, $b \to X_s\gamma$ and Higgs limits in the constrained MSSM, in *Supersymmetry and unification of fundamental interactions: Proceedings*, eds. D.I. Kazakov and A.V. Gladyshev (World Scientific, 2002), p. 196, `hep-ph/0109131`.
44. S. Chen *et al.*, *Phys. Rev. Lett.* **87**, 251807 (2001).
45. P. Koppenburg *et al.*, *Phys. Rev. Lett.* **93**, 061803 (2004).
46. B. Aubert *et al.*, `hep-ex/0207076`.
47. M. Ciuchini, G. Degrassi, P. Gambino and G.F. Giudice, *Nucl. Phys. B* **527**, 21 (1998).
48. M. Ciuchini, G. Degrassi, P. Gambino and G.F. Giudice, *Nucl. Phys. B* **534**, 3 (1998).
49. C. Degrassi, P. Gambino and G.F. Giudice, *JHEP* **0012**, 009 (2000).
50. M. Carena, D. Garcia, U. Nierste and C.E. Wagner, *Phys. Lett. B* **499**, 141 (2001).
51. P. Gambino and M. Misiak, *Nucl. Phys. B* **611**, 338 (2001).
52. D.A. Demir and K.A. Olive, *Phys. Rev. D* **65**, 034007 (2002).
53. F. Borzumati, C. Greub and Y. Yamada, *Phys. Rev. D* **69**, 055005 (2004).
54. T. Hurth, *Rev. Mod. Phys.* **75**, 1159 (2003).
55. W. de Boer, H.J. Grimm, A.V. Gladyshev and D.I.Kazakov, *Phys. Lett. B* **438**, 281 (1998).
56. W. de Boer, M. Huber, A.V. Gladyshev and D.I. Kazakov, The $b \to X_s\gamma$ decay rate in NLO, Higgs boson limits, and LSP masses in the constrained minimal supersymmetric model, in *Proc. 30th International Conference on High-Energy Physics (ICHEP 2000)*, eds. C.S. Lim and T. Yamanaka (World Scientific, 2001), Vol. 2, p. 1086, `hep-ph/0007078`.
57. W. de Boer, M. Huber, A.V. Gladyshev and D.I. Kazakov, *Eur. Phys. J. C* **20**, 689 (2001).
58. The LEP Higgs Working Group, CERN-LHWG-2001-04 and LEP experiments, ALEPH 2001-057, DELPHI 2001-114, L3-Note 2700, OPAL TN699.

59. A.V. Gladyshev, D.I. Kazakov, W. de Boer, G. Burkart and R. Ehret, *Nucl. Phys. B* **498**, 3 (1997).
60. J.R. Ellis, S. Heinemyer, K.A. Olive and G. Weiglein, *Phys. Lett. B* **515**, 348 (2001).
61. J.R. Ellis *et al.*, *Nucl. Phys. B* **238**, 453 (1984).
62. G. Jungman, M. Kamionkowski and K. Griest, *Phys. Rep.* **267**, 195 (1996).
63. M. Drees and M.M. Nojiri, *Phys. Rev. D* **47**, 376 (1993).
64. J.L. Lopez, D.V. Nanopoulos and H. Pois, *Phys. Rev. D* **47**, 2468 (1993).
65. P. Nath and R. Arnowitt, *Phys. Rev. Lett.* **70**, 3696 (1993).
66. L. Roszkowski, R. Ruiz de Austri and T. Nihei, *JHEP* **0108**, 024 (2001).
67. J.R. Ellis, K.A. Olive, Y. Santoso and V.C. Spanos, *Phys. Lett. B* **565**, 176 (2003).
68. W. de Boer and C. Sander, *Phys. Lett. B* **585**, 276 (2004).
69. A. Pukhov, *CalcHEP 3.2: MSSM, structure functions, event generation, batches and generation of matrix elements for other packages*, `hep-ph/0412191`.
70. A.D. Martin, R.G. Roberts, W.J. Stirling, and R.S. Thorne, *Eur. Phys. J. C* **28**, 455 (2003).
71. H. Baer, F. Paige, S.D. Protopescu and X. Tata, *ISAJET 7.69. A Monte Carlo Event Generator for $pp, p\bar{p}$ and e^+, e^- reactions*, `hep-ph/0312045`.
72. V.M. Abazov *et al.* (D0 Collaboration), *Phys. Rev. Lett.* **95**, 151805 (2005).
73. M. Toharia and D. Wells, `hep-ph/0503175`.
74. S.M. Bilenky, *Introduction to Feynman Diagrams and Physics of Electroweak Interactions* (Energoatomizdat, Moscow, 1990), p.163.